Cite this: *INEOS OPEN*, **2023**, *6 (2)*, 49–54
DOI: 10.32931/io2312a

Received 20 September 2023,
Accepted 17 November 2023

http://ineosopen.org

SILVER-CONTAINING COLLAGEN SCAFFOLD: SYNTHESIS AND STRUCTURE

A. N. Tretyakova[a,b] and A. Yu. Vasil'kov*[a]

[a] *Nesmeyanov Institute of Organoelement Compounds, Russian Academy of Sciences, ul. Vavilova 28, str. 1, Moscow, 119334 Russia*
[b] *Moscow Institute of Physics and Technology (National Research University), Institutskiy per. 9, Dolgoprudny, Moscow Region, 141700 Russia*

Abstract

A new metal-containing hybrid material is prepared by the modification of a porous collagen sponge with silver nanoparticles obtained by metal vapor synthesis. Isopropanol is used as a dispersion medium for the production of the silver organosol. The composite is characterized by different physicochemical methods.

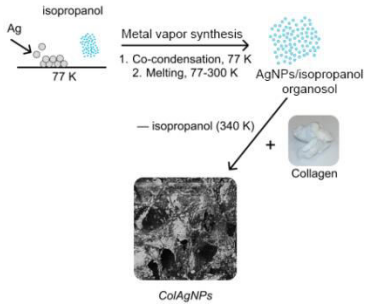

Key words: collagen, nanoparticles, silver, metal vapor synthesis.

Introduction

Environmental issues are among the most serious challenges of the 21st century. One of the actively developing areas that serves to preserve the environment is the use of green technologies and renewable resources.

A large variety of studies have been devoted to the application of renewable resources to obtain new materials [1, 2]. Collagen, chitosan, and bacterial cellulose are nontoxic and biocompatible, which enables the construction of multifunctional hybrid materials on their basis [3–6]. Collagen (Col) is biocompatible with all types of tissues and cells, both within and between species, and is capable of interacting with biologically active components of organic and inorganic nature. To impart new functional properties, collagen is modified with antibiotics, chitosan, various organic substances, as well as metal and metal oxide nanoparticles (NPs) which display biological activity [7–12]. The latter may give rise to a synergistic effect [13].

Various functional materials have been developed based on collagen to date: a collagen-chitosan framework containing Ag and Au nanoparticles [7], collagen-hydroxyapatite matrices with Ag nanoparticles [14], a nanocomposite based on collagen and zinc titanate [15], a metal-organic framework based on cobalt [16], collagen microneedles [17], and dressings based on collagen modified with chitosan nanoparticles with insulin [18]. A number of materials with different substrates have been tested as wound coverings: collagen nanomatrix [19], collagen gel [20, 21], collagen-hydroxyapatite matrices [22], and collagen-chitosan composites [7, 23].

Metal nanoparticles are usually produced by chemical reduction [24], photochemical methods [25], biosynthesis [26, 27] or using UV radiation [28]. For medical materials, it is necessary to create pure composites that do not contain impurities. Most synthetic methods either do not allow achieving the required purity of a product or are too expensive to implement. The chemical reduction methods can lead to the material contamination with nonreduced metal salts, surfactants, and reducing agents. Metal vapor synthesis (MVS) is actively used for the creation of medical materials, since it can provide biologically active metal nanoparticles and functional materials on their basis. The MVS technique allows for avoiding or significantly reducing the contamination of biomedical materials during their production [29–31]. These advantages promote the application of the MVS in the creation of new generation medical materials. Earlier it has been shown that the modification of porous chitosan-based films, which did not exhibit biological activity, with Ag nanoparticles obtained by the MVS provides an effective antibacterial material [32].

It could be expected that the use of the MVS products would also be promising in the creation of biologically active hybrid systems based on other practically important biopolymers. In this work, the MVS technique was used to obtain for the first time the Ag-containing nanocomposites based on collagen in the form of porous materials.

Metal nanoparticles are extremely reactive; therefore, a comprehensive study of promising medical materials using different physicochemical methods is essential for their further use. This report includes the results of a complex analysis of the structure, surface morphology and composition, as well as the electronic state of the metal in the resulting nanocomposite.

Results and discussion

The target metal-containing composites based on collagen were obtained by the MVS technique. Figure 1 depicts a synthetic scheme for the silver-containing collagen sample (ColAgNPs).

Figure 1. Synthesis of ColAgNPs.

Collagen in the form of a porous sponge obtained by the lyophilization of a collagen gel was chosen for the modification (Fig. 2a). The initial collagen samples were obtained by the enzymatic acid extraction from cattle tendons [33, 34].

The modification of Col with the Ag organosol afforded the ColAgNPs sponge. Its analysis revealed a gradient of the metal distribution over the material volume. Despite a porous structure of the initial polymer, its impregnation with the organosol of Ag NPs in isopropanol leads to a significant enrichment of the surface and subsurface layer of the porous material with the metal. Apparently, this is due to both the active chemisorption of silver nanoparticles by the functional groups of Col and the interaction of the metal particles with each other, which prevents them from entering the porous sponge volume (Fig. 2b). The effect of the gradient distribution of the metal may be interesting for the production of film materials for medical purposes, in which the surface plays the role of the determining antibacterial element of the system.

The morphology of Col and ColAgNPs samples was studied using scanning electron microscopy (SEM). The lyophilized collagen represents a porous polymer sponge that has a cellular rather than fibrous structure (Fig. 3). The ColAgNPs sample features an altered surface morphology: silver nanoparticles cover a larger area of collagen fibrils (Fig. 4). The metal atoms are distributed unevenly over the surface; besides Ag nanoparticles, there are also the aggregates that probably have a bunch of grapes structure and consist of smaller particles. This structure for the aggregates obtained by a similar method from an isopropanol–silver organosol during the synthesis of the AgNPs-cotton system was previously established by the high-resolution transmission electron microscopy [29].

The thermogravimetric analysis showed that the mass loss of Col and ColAgNPs in the air occurs in three stages (Fig. 5). During heating to 100 °C, the loss of moisture sorbed from the air occurs [35]. The main decomposition processes take place in the range of 230–400 °C. The presence of Ag nanoparticles in collagen leads to a slight decrease in thermal stability of the system at temperatures from 100 to 350 °C. A subsequent increase in the temperature is accompanied by a decrease in

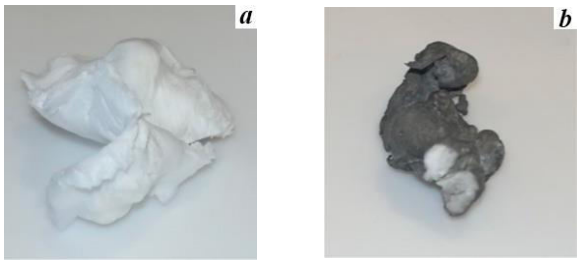

Figure 2. Photographs of the samples: lyophilized collagen (***a***), collagen modified with Ag NPs (***b***).

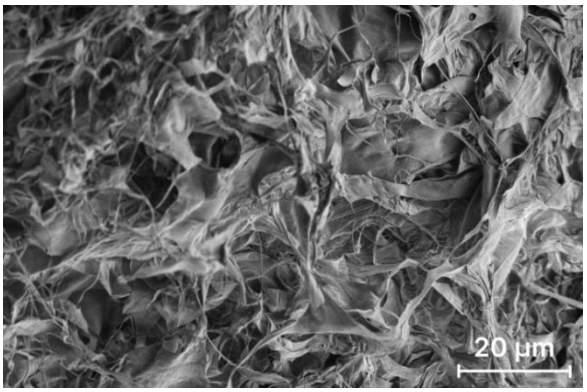

Figure 3. SEM micrograph of the surface of the lyophilized collagen sample.

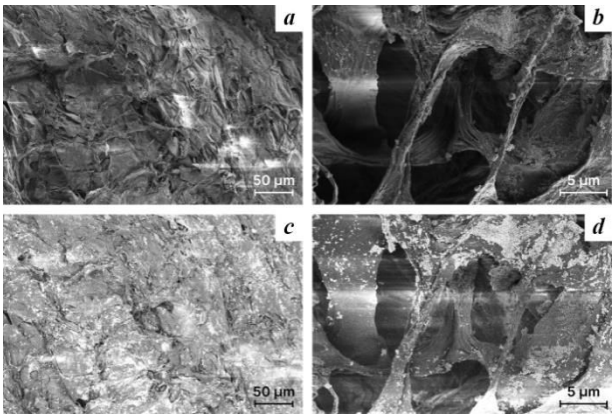

Figure 4. SEM micrographs of the surface of ColAgNPs at magnifications of 50 μm (***a***, ***c***) and 5 μm (***b***, ***d***). Images ***a*** and ***b*** were obtained in the SE mode, images ***c*** and ***d***—in the BSE mode.

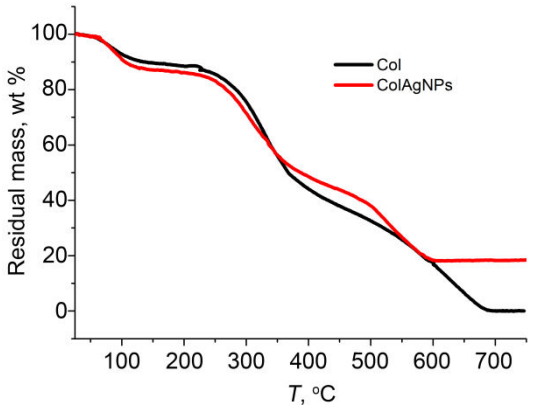

Figure 5. Thermogravimetric curves of collagen and the Ag-containing composite.

the mass loss for the metal-containing system, which can be caused by both the oxidation of Ag nanoparticles and the formation of a more thermally stable metal-carbon residue.

The Col and ColAgNPs samples were analyzed by X-ray diffraction (XRD). The XRD pattern of the initial collagen revealed two peaks: a small one at 2θ around 8° and a broad peak centered with the maximum at about 20° (see Fig. S1 in the Electronic supplementary information (ESI)). The absence of intense reflections in the diffraction pattern of collagen characterizes its X-ray amorphous nature [36]. All the peaks observed in the XRD pattern of ColAgNPs are attributed to an FCC packing of silver nanoparticles (Fig. 6). The peaks were observed at the following values of 2θ: 38.1° (111), 44.3° (002), 64.5° (022), 77.4° (311), and 81.5° (222). The size of metal nanoparticles in the ColAgNPs sample, estimated using the Scherrer formula, was 11 nm.

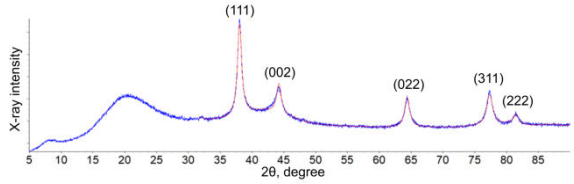

Figure 6. X-ray diffraction pattern of the ColAgNPs composite.

The surface composition plays a key role in the biological and catalytic activity of metal nanoparticles. It was shown earlier that the surface of metal nanoparticles synthesized by the MVS technique are coated with a hydrocarbon shell which does not affect their biological activity [37–39]. The initial and metal-containing collagen samples were studied by X-ray photoelectron spectroscopy, which is a leading method for analyzing various chemical/physical forms of elements in the surface of materials. From the full spectra of the samples (Fig. S2 in the ESI), the relative atomic concentrations of the elements were determined (Table 1).

Table 1. Relative atomic concentrations of the elements according to the results of the XPS analysis

Sample/element	C	N	O	Ag
Col	52	15	32	–
ColAgNPs	44	13	17	26

Collagen is represented by repeating Gly-Pro-Hyp amino acid sequences [40], therefore, ideally, the C 1s spectrum should contain the following states: C–C/C–H, C–N–H, C–OH, O*–C=O, N–C=O, and O–C=O* [41]. No more than four states are usually used to describe the XPS spectra [42, 43]. This is due to the fact that the range of chemical shifts of the C–N–H, C–O–C, C–OH, and O*–C=O bonds largely overlaps [41] and therefore, to simplify the spectrum, a number of peaks can be replaced for a total peak [44]. In the case of the Col and ColAgNPs samples, the C 1s spectra had similar shapes (Fig. 7).

The minor differences in the binding energies can be attributed to the effect of sample charging during the acquisition process (Table 2). The differences in the content of amide groups that are key to protein structures are likely to be associated with the effect of Ag nanoparticles on the biopolymer.

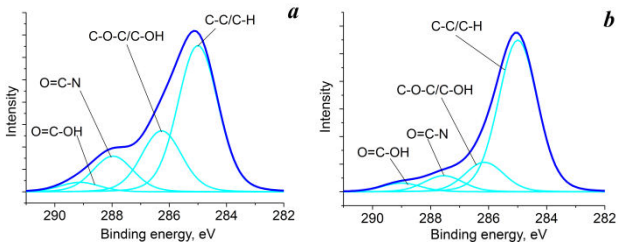

Figure 7. High-resolution C 1s photoelectron spectra of the Col (***a***) and ColAgNPs (***b***) samples.

Table 2. Characteristics of the C 1s photoelectron spectra: binding energies (E_b), widths (W), and relative intensities (I_{rel}) of the photoelectron peaks

	Group	C–C/ C–H	C–O–C/ C–OH	O=C–N	O=C–OH
Col	E_b, eV	285.00	286.27	287.97	289.12
	W, eV	1.65	1.65	1.65	1.65
	I_{rel}, %	57.98	24.17	14.12	3.73
ColAgNPs	E_b, eV	285.00	286.15	287.55	289.00
	W, eV	1.58	1.58	1.58	1.58
	I_{rel}, %	73.68	14.32	7.78	4.22

A typical N 1s spectrum of collagen is described by three ground states C–NH_2, O=C–N, and C–NH_3^+ with the binding energies of 399.6, 400.5, and 401.3 eV, respectively [41, 45]. In the case of the ColAgNPs spectrum, a decrease in the content of the amide groups was detected, which was identical to the changes in the C 1s spectrum. This may be due to both damage of the peptide chain and the interaction of collagen with Ag NPs (Fig. 8, Table 3).

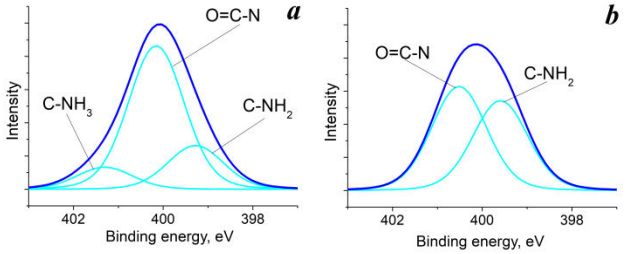

Figure 8. High-resolution N 1s photoelectron spectra of the Col (***a***) and ColAgNPs (***b***) samples.

Table 3. Characteristics of the N 1s photoelectron spectra: binding energies (E_b), widths (W), and relative intensities (I_{rel}) of the photoelectron peaks

	Group	O=C–N	C–NH_2	C–NH_3^+
Col	E_b, eV	400.15	399.28	401.30
	W, eV	1.46	1.46	1.46
	I_{rel}, %	68.55	20.91	10.54
ColAgNPs	E_b, eV	400.52	399.59	–
	W, eV	1.45	1.45	–
	I_{rel}, %	53.66	46.34	–

Figure 9 shows the high-resolution Ag 3d spectrum. The latter shows a characteristic spin splitting of 6 eV, as well as plasmon loss peaks corresponding to the binding energies of 371.84 and 377.84 eV. The binding energies of the Ag $3d_{5/2}$ and Ag $3d_{3/2}$ peaks differ from the average values characteristic of zero-valent silver 368.2 and 374.2 eV [46]. This difference may be caused by a size effect [47]. The value of the modified Auger parameter α' = 726.47 eV also indicates the Ag^0 state [48]. The presence of plasmon loss peaks, given the size effect and the value of the Auger parameter, allows us to conclude that Ag nanoparticles in the composite are in a zero-valent state.

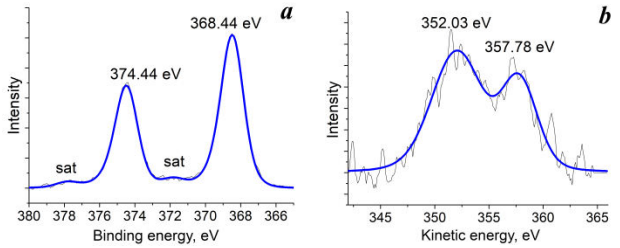

Figure 9. High-resolution Ag 3d photoelectron (***a***) and Ag MNN Auger (***b***) spectra of ColAgNPs.

Experimental section

Silver nanoparticles were prepared by the MVS technique from isopropanol (Aldrich, 99.7%) and silver (99.99%). Lyophilized dry collagen was synthesized at the Interuniversity Research Laboratory of the Tashkent Medical Academy, Uzbekistan [33, 34].

The surface morphology of the initial and modified collagen samples was studied by low-voltage scanning electron microscopy on an FEI Scios microscope (Thermo Fisher Scientific, Waltham, MA, USA) in the secondary and backscattered electron modes with an accelerating voltage of less than 1 kV.

The thermal stability of the materials was studied by thermogravimetric analysis using a MOM unit (Hungary) heating in the air with a rate of 10 °C/min to 750 °C.

The XRD analysis was performed on a D8 Advance diffractometer (Bruker AXS) in Bragg–Brentano focusing geometry using CuKα radiation, an angle range of 5–90° with a step of 0.02°, and a scanning rate of 0.5–2 deg/min. The X-ray diffraction patterns were fitted using the TOPAS 5 package (Bruker AXS).

The X-ray photoelectron spectra were recorded using a monochromatic Al Kα X-ray source with a photon energy of 1486.6 eV on a Thermo Fisher Scientific Theta Probe instrument. The measurements were carried out at room temperature and a chamber pressure of 5×10^{-10} mbar. The binding energy scale was calibrated using the Au $4f_{7/2}$ (83.96 ± 0.02 eV), Ag $3d_{5/2}$ (368.21 ± 0.02 eV), and Cu $2p_{3/2}$ (932.62 ± 0.02 eV) peaks. The spectra were recorded in the constant energy mode of the analyzer. The full spectra were registered with the transmission energy of 300 eV, the step of 1 eV, the delay time of 0.05 s, and the number of scans of 5. The high-resolution spectra were recorded with the transmission energy of 100 eV, the step of 0.1 eV, the delay time of 0.1 s, and the number of scans of 15 [46]. The quantitative analysis was performed using the full spectrum and elemental sensitivity coefficients included in the spectrometer software.

Metal vapor synthesis of the silver nanoparticles. Isopropanol (Aldrich, 99.7%) was dried over 4 Å molecular sieves and distilled under an argon atmosphere. The MVS unit and experimental procedure are described elsewhere [29, 37]. The metal was evaporated from a resistive evaporator, which was a 90 × 5.5 mm tantalum boat made of 0.25 mm thick foil. Using a high-vacuum diffusion pump (VA-01-1 vacuum unit, Russia), a pressure of 10^{-2} Pa was created in a five-liter glass quartz reactor.

The flask with isopropanol was connected to the organic reagent supply line and degassed under vacuum by alternating freeze/thaw cycles. The rate of the organic reagent supply was controlled by a fine adjustment valve. The synthesis involved the combined condensation of Ag and isopropanol vapors on the reactor walls cooled to 77 K. The experiment was performed with 120 mL of the organic reagent and 0.2 g of the metal. After its completion, the cooling bath was removed and the reactor was filled with argon. As the temperature increases, the matrix melts, forming a colloidal solution of Ag nanoparticles in isopropanol.

Synthesis of the collagen-based composite. The modification of a collagen sponge was carried out *in situ*: the resulting organosol was extracted from the reactor into an evacuated flask containing lyophilized dry collagen using a siphon system. The mixture was stirred with a magnetic stirrer at room temperature for 1 h, then the flask was filled with argon and disconnected from the siphon line. The excess organosol was removed, and the ColAgNPs product was dried to constant mass at 60 °C and 10^{-1} Pa.

Conclusions

The method was developed for the ecologically friendly synthesis of the collagen-based hybrid systems in the form of films, sponges, and powders containing biologically active metal nanoparticles. The scanning electron microscopy and X-ray photoelectron spectroscopy studies revealed that the modification of collagen with silver nanoparticles significantly changes the morphology and composition of the polymer surface. It was established that silver in the material is in the Ag^0 state, and the average size of the nanoparticles is about 11 nm.

The results obtained demonstrate the possibilities of using green MVS method to obtain composites based on collagen and silver nanoparticles as promising materials for medical purposes, for example, wound care dressings.

Acknowledgements

The work was performed with financial support from the Ministry of Science and Higher Education of the Russian Federation (agreement no. 075-00277-24-00) using the equipment of the Center for Molecular Composition Studies of INEOS RAS.

The authors are grateful to M. I. Buzin, A. S. Golub, and A. Yu. Pereyaslavtsev for help in analyzing the materials and N. E. Tseomashko for providing the collagen samples.

Corresponding author

* E-mail: alexandervasilkov@yandex.ru (A. Yu. Vasil'kov)

Electronic supplementary information

Electronic supplementary information (ESI) available online: X-ray diffraction pattern of collagen; full photoelectron spectra of the Col and ColAgNPs samples. For ESI, see DOI: 10.32931/io2312a

References

1. M. Ojeda-Martínez, I. Yáñez-Sánchez, C. Velásquez-Ordoñez, M. M. Martínez-Palomar, A. Álvarez-Rodríguez, M. A. Garcia-Sánchez, F. Rojas-González, F. J. Gálvez-Gastélum, *J. Bioact. Compat. Polym.*, **2015**, *30*, 617–632. DOI: 10.1177/0883911515590495
2. S. Gorgieva, J. Trček, *Nanomaterials*, **2019**, *9*, 1352. DOI: 10.3390/nano9101352
3. N. E. Tseomashko, M. Rai, A. Yu. Vasil'kov, in: *Biopolymer-Based Nano Films. Applications in Food Packaging and Wound Healing*, M. Rai, C. Alves dos Santos (Eds.), Elsevier, Amsterdam, Oxford, Cambridge, **2021**, ch. 12, pp. 203–246. DOI: 10.1016/B978-0-12-823381-8.00007-7
4. A. B. Shekhter, A. L. Fayzullin, M. N. Vukolova, T. G. Rudenko, V. D. Osipycheva, P. F. Litvitsky, *Curr. Med. Chem.*, **2019**, *26*, 506–516. DOI: 10.2174/0929867325666171205170339
5. R. Dong, B. Guo, *Nano Today*, **2021**, *41*, 101290. DOI: 10.1016/j.nantod.2021.101290
6. S. S. Mathew-Steiner, S. Roy, C. K. Sen, *Bioengineering*, **2021**, *8*, 63. DOI: 10.3390/bioengineering8050063
7. M. S. Rubina, E. E. Said-Galiev, A. V. Naumkin, A. V. Shulenina, O. A. Belyakova, A. Yu. Vasil'kov, *Polym. Eng. Sci.*, **2019**, *59*, 2479–2487. DOI: 10.1002/pen.25122
8. R. Shah, P. Stodulka, K. Skopalova, P. Saha, *Polymers*, **2019**, *11*, 2094. DOI: 10.3390/polym11122094
9. N. N. Fathima, B. Madhan, J. R. Rao, B. U. Nair, T. Ramasami, *Int. J. Biol. Macromol.*, **2004**, *34*, 241–247. DOI: 10.1016/j.ijbiomac.2004.05.004
10. D. M. Júnior, M. A. Hausen, J. Asami, A. M. Higa, F. L. Leite, G. P. Mambrini, A. L. Rossi, D. Komatsu, E. A. de Rezende Duek, *Antibiotics*, **2021**, *10*, 742. DOI: 10.3390/antibiotics10060742
11. B. Kaczmarek, O. Mazur, *Materials*, **2020**, *13*, 3641. DOI: 10.3390/ma13163641
12. L. G. Wasef, H. M. Shaheen, Y. S. El-Sayed, T. I. A. Shalaby, D. H. Samak, M. E. Abd El-Hack, A. Al-Owaimer, I. M. Saadeldin, A. El-mleeh, H. Ba-Awadh, A. A. Swelum, *Biol. Trace Elem. Res.*, **2020**, *193*, 456–465. DOI: 10.1007/s12011-019-01729-z
13. X. Xie, C. Mao, X. Liu, Y. Zhang, Z. Cui, X. Yang, K. W. K. Yeung, H. Pan, P. K. Chu, S. Wu, *ACS Appl. Mater. Interfaces*, **2017**, *9*, 26417–26428. DOI: 10.1021/acsami.7b06702
14. I. V. Antoniac, A. Antoniac, E. Vasile, C. Tecu, M. Fosca, V. G. Yankova, J. V. Rau, *Bioact. Mater.*, **2021**, *6*, 3383–3395. DOI: 10.1016/j.bioactmat.2021.02.030
15. M. G. Albu, T. G. Vladkova, I. A. Ivanova, A. S. A. Shalaby, V. S. Moskova-Doumanova, A. D. Staneva, Y. B. Dimitriev, A. S. Kostadinova, T. I. Topouzova-Hristova, *Appl. Biochem. Biotechnol.*, **2016**, *180*, 177–193. DOI: 10.1007/s12010-016-2092-x
16. J. Li, F. Lv, J. Li, Y. Li, J. Gao, J. Luo, F. Xue, Q. Ke, H. Xu, *Nano Res.*, **2020**, *13*, 2268-2279. DOI: 10.1007/s12274-020-2846-1
17. A. Aditya, B. Kim, R. D. Koyani, B. Oropeza, M. Furth, J. Kim, N. P. Kim, *J. Drug Delivery Sci. Technol.*, **2019**, *52*, 618–623. DOI: 10.1016/j.jddst.2019.03.007
18. A. Ehterami, M. Salehi, S. Farzamfar, A. Vaez, H. Samadian, H. Sahrapeyma, M. Mirzaii, S. Ghorbani, A. Goodarzi, *Int. J. Biol. Macromol.*, **2018**, *117*, 601–609. DOI: 10.1016/j.ijbiomac.2018.05.184
19. G. Rath, T. Hussain, G. Chauhan, T. Garg, A. K. Goyal, *J. Drug Targeting*, **2016**, *24*, 520–529. DOI: 10.3109/1061186X.2015.1095922
20. E. I. Alarcon, B. Vulesevic, A. Argawal, A. Ross, P. Bejjani, J. Podrebarac, R. Ravichandran, J. Phopase, E. J. Suuronen, M. Griffith, *Nanoscale*, **2016**, *8*, 6484–6489. DOI: 10.1039/C6NR01339B
21. P. Preda, A.-M. Enciu, B. Adiaconita, I. Mihalache, G. Craciun, A. Boldeiu, L. Aricov, C. Romanitan, D. Stan, C. Marculescu, C. Tanase, M. Avram, *Gels*, **2022**, *8*, 604. DOI: 10.3390/gels8100604
22. A. Salleh, N. Mustafa, Y. H. Teow, M. N. Fatimah, F. A. Khairudin, I. Ahmad, Mh B. Fauzi, *Biomedicines*, **2022**, *10*, 816. DOI: 10.3390/biomedicines10040816
23. P. E. Antezana, S. Municoy, C. J. Pérez, M. F. Desimone, *Antibiotics*, **2021**, *10*, 1420. DOI: 10.3390/antibiotics10111420
24. J. M. Patrascu, I. A. Nedelcu, M. Sonmez, D. Ficai, A. Ficai, B. S. Vasile, C. Ungureanu, M. G. Albu, B. Andor, E. Andronescu, L. C. Rusu, *J. Nanomater.*, **2015**, *2015*, 587989. DOI: 10.1155/2015/587989
25. E. I. Alarcon, K. Udekwu, M. Skog, N. L. Pacioni, K. G. Stamplecoskie, M. González-Béjar, N. Polisetti, A. Wickham, A. Richter-Dahlfors, M. Griffith, J. C. Scaiano, *Biomaterials*, **2012**, *33*, 4947–4956. DOI: 10.1016/j.biomaterials.2012.03.033
26. R. F. Talabani, S. M. Hamad, A. A. Barzinjy, U. Demir, *Nanomaterials*, **2021**, *11*, 2421. DOI: 10.3390/nano11092421
27. A. Yu. Vasil'kov, K. A. Abd-Elsalam, A. Yu. Olenin, in: *Green Synthesis of Silver Nanomaterials. Nanobiotechnology for Plant Protection*, K. A. Abd-Elsalam (Ed.), Elsevier, Amsterdam, Oxford, Cambridge, **2022**, ch. 10, pp. 241–281. DOI: 10.1016/B978-0-12-824508-8.00028-9
28. Z. Yu, W. Wang, R. Dhital, F. Kong, M. Lin, A. Mustapha, *Colloids Surf., B*, **2019**, *180*, 212–220. DOI: 10.1016/j.colsurfb.2019.04.054
29. A. Yu. Vasil'kov, R. I. Dovnar, S. M. Smotryn, N. N. Iaskevich, A. V. Naumkin, *Antibiotics*, **2018**, *7*, 80. DOI: 10.3390/antibiotics7030080
30. D. Barbaro, L. Di Bari, V. Gandin, C. Marzano, A. Ciaramella, M. Malventi, C. Evangelisti, *PLoS One*, **2022**, *17*, e0269603. DOI: 10.1371/journal.pone.0269603
31. G. Cárdenas-Triviño, C. Elgueta, L. Vergara, J. Ojeda, A. Valenzuela, C. Cruzat, *Int. J. Biol. Macromol.*, **2017**, *104*, 498–507. DOI: 10.1016/j.ijbiomac.2017.06.040
32. RU Patent 2804241, **2023**.
33. KZ Patent 30528, **2015**.
34. KZ Patent 23370, **2010**.
35. B. T. Mekonnen, M. Ragothaman, T. Palanisamy, *ACS Omega*, **2017**, *2*, 5260–5270. DOI: 10.1021/acsomega.7b01011
36. T.-W. Sun, Y.-J. Zhu, F. Chen, *RSC Adv.*, **2018**, *8*, 26218–26229. DOI: 10.1039/C8RA03972K
37. A. A. Voronova, A. V. Naumkin, A. Yu. Vasil'kov, *INEOS OPEN*, **2022**, *5*, 79–84. DOI: 10.32931/io2215a
38. A. Vasil'kov, T. Batsalova, B. Dzhambazov, A. Naumkin, *Surf. Interface Anal.*, **2022**, *54*, 189–202. DOI: 10.1002/sia.7038
39. A. Vasil'kov, A. Voronova, T. Batsalova, D. Moten, A. Naumkin, E. Shtykova, V. Volkov, I. Teneva, B. Dzhambazov, *Materials*, **2023**, *16*, 3238. DOI: 10.3390/ma16083238
40. A. Owczarzy, R. Kurasiński, K. Kulig, W. Rogóż, A. Szkudlarek, M. Maciążek-Jurczyk, *Eng. Biomater.*, **2020**, *156*, 17–23. DOI: 10.34821/eng.biomat.156.2020.17-23
41. G. Beamson, D. Briggs, *High Resolution XPS of Organic Polymers. The Scienta ESCA300 Database*, Wiley, Chichester, New York, **1992**.
42. P. Gentile, K. McColgan-Bannon, N. C. Gianone, F. Sefat, K. Dalgarno, A. M. Ferreira, *Materials*, **2017**, *10*, 693. DOI: 10.3390/ma10070693

43. A. Sionkowska, M. Wisniewski, H. Kaczmarek, J. Skopinska, P. Chevallier, D. Mantovani, S. Lazare, V. Tokarev, *Appl. Surf. Sci.*, **2006**, *253*, 1970–1977. DOI: 10.1016/j.apsusc.2006.03.048
44. T. R. Gengenbach, G. H. Major, M. R. Linford, C. D. Easton, *J. Vac. Sci. Technol., A.*, **2021**, *39*, 013204. DOI: 10.1116/6.0000682
45. G. Zambonin, I. Losito, J. T. Triffitt, C. G. Zambonin, *J. Biomed. Mater. Res.*, **2000**, *49*, 120–126. DOI: 10.1002/(SICI)1097-4636(200001)49:1<120::AID-JBM15>3.0.CO;2-Q
46. G. Beamson, D. Briggs, *The XPS of Polymers. Database*, SurfaceSpectra, Manchester UK, **2000**.
47. G. K. Wertheim, S. B. DiCenzo, D. N. E. Buchanan, *Phys. Rev. B*, **1986**, *33*, 5384–5390. DOI: 10.1103/PhysRevB.33.5384
48. S. Bera, P. Gangopadhyay, K. G. M. Nair, B. K. Panigrahi, S. V. Narasimhan, *J. Electron Spectrosc. Relat. Phenom.*, **2006**, *152*, 91–95. DOI: 10.1016/j.elspec.2006.03.008